Impact of Volcanic Aerosols on Stratospheric Ozone Recovery

Short/Running Title: Impact of volcanic aerosols on stratospheric O_3

Vaishali Naik[1], Larry W. Horowitz[2], and M. Daniel Schwarzkopf[2]

[1] UCAR/NOAA Geophysical Fluid Dynamics Laboratory, Princeton, NJ 08540

[2] NOAA Geophysical Fluid Dynamics Laboratory, Princeton, NJ 08540

Corresponding Author: V. Naik (Vaishali.Naik@noaa.gov)

Keywords: stratospheric volcanic aerosols, ozone recovery, RCP8.5

Geophysical Research Letters, October 2014.

Key Points:

- Volcanic aerosols modulate future evolution of stratospheric O_3
- Stratospheric O_3 recovers earlier in the presence of volcanic aerosols
- Projections of stratospheric O_3 should consider volcanic aerosols

Abstract

We show that the uncertainty in predicting stratospheric ozone (O_3) recovery from volcanic aerosols in the coming decades can be accounted for by including volcanic aerosol loading similar to that observed over the last decade in simulations projecting the future abundance of stratospheric O_3. The recent multi-model assessment of stratospheric O_3 projections did not consider any changes in stratospheric aerosols from volcanoes after the year 2000. Analysis of 21st century transient chemistry-climate model simulations with and without aerosol loadings indicates that volcanic aerosols delay the recovery of stratospheric O_3 column in the 2000-2020 period characterized by high atmospheric halogen abundance. However, as halogen levels decline O_3 recovers to 1980 levels about seven years earlier in the presence of volcanic aerosols relative to that in their absence. Our results illustrate that natural volcanic aerosols modulate the future evolution of stratospheric O_3, inducing uncertainty in estimates of future O_3 recovery.

1. Introduction

Perturbations in stratospheric aerosols affect stratospheric ozone (O_3) directly via changes in heterogeneous chemistry and photolysis rates and indirectly via changes in stratospheric temperature and large-scale circulation patterns [*SPARC* 2006]. Recent measurements indicate that there has been a discrete increase in stratospheric aerosols in the last decade following a period (1998-2002) of background (non-volcanic) stratospheric aerosol levels, which has been attributed to smaller but intense tropical volcanic eruptions [*Vernier et al.,* 2011]. Volcanic aerosols were set to zero or near-zero background in the Coupled Model Intercomparison Project Phase 5 (CMIP5) global chemistry-climate model simulations over the future (2006-2100) period [*Collins et al.,* 2014; see their Table 12.1]. Thus, the impact of volcanic perturbations on the evolution of stratospheric O_3 in the 21st century is generally neglected in multi-model projections [*Eyring et al.*, 2013]. Here we explore the evolution of stratospheric O_3 for the 2006-2100 time period in response to a constant volcanic aerosol loading with the goal of highlighting the importance of considering this important natural perturbation on stratospheric O_3 recovery.

Volcanic eruptions enhance the background stratospheric aerosol layer, first identified by *Junge et al.* [1961], by injecting large amounts of sulfur dioxide (SO_2). SO_2 oxidizes to sulfuric acid (H_2SO_4) which nucleates homogeneously or condenses on existing particles to form sulfate aerosols (H_2SO_4-H_2O). Volcanic sulfate aerosols affect the Earth's radiative balance by increasing the scattering of incoming solar radiation and enhancing the infrared absorption depending on the particle size, thus cooling the troposphere and warming the stratosphere [*McCormick et al.* 1995]. Recent ground-based measurements show an increasing trend in background stratospheric aerosols of 4-7% per year over the period 2000-2009 [*Hofmann et al.* 2009]. Satellite measurements confirm this increase, and attribute it to largely smaller but more

intense tropical volcanic eruptions [*Vernier et al.* 2009; 2011]. Recent work has emphasized the importance of increasing volcanic stratospheric aerosols since 2000 on climate [*Solomon et al*., 2011; *Fyfe et al.* 2013; *Haywood et al.*, 2013; *Santer et al.*, 2014]. These changes in volcanic stratospheric aerosols can impact stratospheric O_3 via heterogeneous chemistry as discussed below.

Observational and modeling studies after the Pinatubo eruption have provided evidence that heterogeneous chemistry on stratospheric aerosols modulates the abundance of stratospheric O_3 [see *Solomon et al.* 1999 for a detailed review]. Enhanced aerosol loading following volcanic eruptions reduce the NO_x/NO_y partitioning [*Fahey et al.*, 1993], resulting in suppressed NO_x-catalyzed O_3 loss particularly in the middle stratosphere where the NO_x cycle is efficient at destroying O_3 [*Brasseur et al.* 1999]. This control of NO_x by stratospheric aerosols is more pronounced at low aerosol loading since the NO_x effect saturates as aerosol surface area increases beyond about 10 μm^2 cm^{-3} [*Prather*, 1992; *Fahey et al.* 1993]. Increased volcanic aerosol loading also increases the efficiency of O_3 destruction by halogen (chlorine and bromine) and HO_x cycles [*Wennberg et al.*, 1994; *Lary et al.*, 1996; *Solomon et al.*, 1996]. The net impact of enhanced volcanic aerosols in the contemporary atmosphere is to increase O_3 in the middle stratosphere and decrease O_3 in the lower stratosphere, with the overall effect on global O_3 burden depending on the halogen loading of the atmosphere [*Tie and Brasseur,* 1995]. Indeed, *Austin et al.* [2013] find that volcanic eruptions in the pre-halogen era led to a temporary increase in ozone column while those in the presence of anthropogenic halogen caused O_3 column to decrease.

Long-term changes in stratospheric O_3 over the historical (1850-2005) and future (2006-2100) time periods were assessed from the chemistry-climate model (CCM) simulations

conducted in support of CMIP5 [*Eyring et al.,* 2013]. Nine of the 46 CMIP5 models considered by *Eyring et al*. simulate stratospheric and tropospheric ozone chemistry interactively. Volcanic aerosols in the CMIP5 future simulations following the Representative Concentration Pathway (RCP) scenarios conducted by four of these nine models were set to zero or near-zero background after 2000 [*Collins et al.,* 2014; Table 12.1]. Increasing stratospheric volcanic aerosols after year 2000 will likely have influenced O_3 concentrations and will continue to do so if volcanic aerosols increase in the future. The possibility of significant changes in background aerosols levels has been identified to be a key uncertainty in predicting future O_3 abundance by the World Meteorological Organization and United Nations Environment Programme Scientific Assessment of Ozone Depletion [*Bekki et al.,* 2011]. In this study, we attempt to shed light on the evolution of stratospheric O_3 in response to a non-zero volcanic aerosol loading in the 2000-2100 time period using a global chemistry-climate model.

2. Model and Simulations

We analyze the transient 21st century simulations of the fully interactive chemistry-climate model CM3 [*Donner et al.,* 2011; *Austin et al.,* 2013; *Naik et al.,* 2013]. The chemical mechanism in CM3 includes both tropospheric and stratospheric processes coupled seamlessly [*Austin et al*., 2013; *Naik et al*., 2013]. Stratospheric chemistry, based on *Austin and Wilson* [2010], includes gas-phase reactions describing the HO_x, NO_x, ClO_x, and BrO_x catalytic cycles and heterogeneous reactions on polar stratospheric clouds (PSCs) and ternary liquid particles. Total column O_3 in the historical CM3 simulations in the present-day atmosphere has been shown to generally match the observations, except for a high bias in the tropics and southern mid-latitudes [*Austin et al.,* 2013]. The positive bias in the southern mid-latitudes is likely due to

104 increased strength of the Brewer Dobson circulation transporting more O_3 from the tropics,
105 where O_3 is already high, to the mid-latitudes [*Austin et al.,* 2013; *Eyring et al.,* 2013]. These
106 deficiencies in the model will most likely have minor impact on our results as we discuss relative
107 changes.

108 Direct injection of aerosols or their precursors into the stratosphere is not considered
109 explicitly as the stratospheric aerosol life cycle is not represented in the model. Instead, the effect
110 of stratospheric volcanic aerosols is accounted for by implementing vertically resolved spatial
111 and temporal distributions of volcanic aerosol optical properties (monthly mean aerosol
112 extinction, single scattering albedo, and asymmetry factor). This dataset was originally
113 developed for the Pinatubo eruption based on satellite measurements [*Stenchikov et al.* 1998] and
114 extended to cover the historical time period (1850-1999) based on volcanic aerosol optical
115 depths from *Sato et al*. [1993] and its updates. Volcanic aerosol surface area density (SAD) is
116 derived from aerosol extinction centered at 1.0-μm following the relationship of *Thomason et al.*
117 [1997].

118 We analyze results from two 3-member ensemble transient simulations of CM3
119 conducted for the 2006-2100 time period in which concentrations of greenhouse gases and ozone
120 depleting substances (ODSs), and emissions of short-lived species evolve following the RCP 8.5
121 scenario [*Riahi et al.,* 2011]. Initial conditions for both ensembles are from the respective
122 members of the historical CM3 simulation [*Austin et al.,* 2013]. In the first ensemble,
123 stratospheric volcanic aerosols are set to zero for chemistry and radiation (RCP8.5_novolc). This
124 simulation is different from the CMIP5 RCP8.5 simulation analyzed previously [*Santer et al.,*
125 2012; *John et al.,* 2012; *Eyring et al.,* 2013] in which aerosol surface area for chemistry
126 calculations was inadvertently set to non-zero values. The second ensemble is the same as

RCP8.5_novolc but with stratospheric volcanic aerosols set to 1860 levels (RCP8.5_volc) intended to mimic an arbitrary stratospheric volcanic aerosol distribution greater than zero. The aerosol optical properties derived for January through December of 1860 are repeated over the 95 years of RCP8.5_volc. Since our intention is to assess the sensitivity of stratospheric O_3 to non-zero stratospheric aerosol loading in the future, we set the values to 1860 to represent conditions significantly different from those in RCP8.5_novolc simulation.

The global annual mean volcanic aerosol optical depth in RCP8.5_volc in the visible wavelength is 0.007 which is close to the mean observed AOD over the 2000-2010 period [*Vernier et al*. 2011]. Annual average zonal mean volcanic aerosol SAD in the RCP8.5_volc simulation is shown in Figure S1.

For the analysis discussed below, we average results across ensemble members to better isolate the forced response to volcanic aerosols. Stratospheric O_3 column is defined here as O_3 concentrations integrated above 200 hPa.

3. Impact of Volcanic Aerosols on Stratospheric Ozone

3.1. Ozone Column

We first analyze the long term evolution of stratospheric O_3 column relative to 1980 levels in the RCP8.5_novolc and RCP8.5_volc runs, since return of O_3 to mean 1980 values is a major milestone in the future evolution of O_3 [*Bekki et al.,* 2011]. Figure 1 shows the 1980 baseline-adjusted time series of stratospheric O_3 column from 1960 to 2100 for the RCP8.5_novolc and RCP8.5_volc simulations for globally and in five selected latitude bands. The time series are smoothed with a 1:2:1 filter applied 30 times iteratively [see *Eyring et al*., 2010] to reduce year-to-year variability. The recovery in annual mean global average

150 stratospheric O_3 column is slower for RCP8.5_volc than that for RCP8.5_novolc in the 2000-
151 2020 period (Figure 1a). The two projections intersect in the mid-2020s with O_3 recovering to
152 1980 levels in RCP8.5_volc seven years earlier (2049) than in RCP8.5_novolc (2056). By 2100,
153 the recovery of global stratospheric O_3 column above 1980 levels is 3.5 DU or 45% greater in
154 RCP8.5_volc relative to RCP8.5_novolc and this difference is statistically significant to 1-
155 standard deviation as indicated by the non-overlapping shaded areas in Figure 1a. In the tropics,
156 the annual mean stratospheric O_3 column does not recover to 1980 levels (Figure 1b) in either
157 simulation; however, the baseline-adjusted O_3 column is greater in RCP8.5_volc than in
158 RCP8.5_novolc simulation throughout the 21st century. The non-recovery of tropical
159 stratospheric O_3 column to 1980 levels is consistent with previous multi-model assessments
160 [*Eyring et al*., 2013].

161 In the mid-latitudes, the RCP8.5_novolc and RCP8.5_volc projections of the 1980
162 baseline adjusted annual stratospheric O_3 column (Figures 1c and 1d) evolve in a similar manner
163 as that for global mean. The O_3 column decrease is slightly greater in the presence of volcanic
164 aerosols than in their absence in the early 21st century in both the hemispheres (more so in the
165 southern mid-latitudes). However, by the end of the 21st century O_3 column in RCP8.5_volc
166 surpasses that in RCP8.5_novolc by as much as 6 DU. O_3 recovers to 1980 levels earlier in
167 RCP8.5_volc than in RCP8.5_novolc, with a more pronounced effect in the northern mid-
168 latitudes. The presence of volcanic aerosols has a strong impact on the evolution of stratospheric
169 O_3 column in the polar regions as indicated by the strong reduction in O_3 column in March
170 (Figure 1e) and October (Figure 1f) for northern and southern hemisphere, respectively. The
171 recovery to 1980 levels in RCP8.5_volc is 9-10 years later than that in RCP8.5_novolc in the
172 polar regions. Polar spring time stratospheric O_3 column in RCP8.5_volc surpasses that in

RCP8.5_novolc only in late 21st century (2070s) with values at 2100 for both the simulations not significantly different from each other.

3.2. Vertical Distribution of Zonal Mean Ozone Concentration

To decipher the trends in the stratospheric O_3 columns, we analyze the difference in the zonal mean O_3 concentrations simulated for RCP8.5_novolc and RCP8.5_volc. Left and right columns of Figure 2 show the change in zonal mean O_3 concentrations in RCP8.5_volc relative to RCP8.5_novolc for 2006-2015 and 2091-2100 time periods, respectively; stippling indicates results significant at 95% confidence level based on student's t-test. In the presence of volcanic aerosols, annual mean O_3 concentrations increase by up to 0.3 ppm (5%) throughout the middle stratosphere and decrease by up to 0.3 ppm (20%) in the lower stratosphere over the mean 2006-2015 period (Figure 2, top left); a time period when stratospheric halogen loading is still sufficiently high (as shown by the 1980 baseline-adjusted equivalent stratospheric chlorine in Figure S2). Stronger monthly mean O_3 increases and decreases are simulated in the presence of volcanic aerosols for middle and lower stratosphere, respectively, for northern hemisphere extra-tropics in March (Figure 2, middle left) and southern hemisphere in October (Figure 2, bottom left) when chemistry is more active in these regions. The presence of volcanic aerosols leads to significant O_3 decreases in the polar regions where cold temperatures make heterogeneous chemistry (discussed below) very effective in perturbing O_3. In contrast, in the 2091-2100 period when halogen loading is significantly diminished, the model predicts weaker O_3 decreases in the lower stratosphere but the strong increases in middle stratosphere persist and the spatial extent of statistically significant increases is enhanced for both annual mean and monthly mean changes (Figure 2, right).

3.3. Changes in Chemical Partitioning

We further analyze the changes in stratospheric O_3 by examining the changes in chemical partitioning of reactive nitrogen, NO_y, reactive chlorine, Cl_y, and reactive bromine, Br_y, as a function of volcanic SADs in RCP8.5_novolc and RCP8.5_volc, focusing on the northern mid-latitudes. Observed dependencies of NO_x/NO_y, ClO/Cl_y, HNO_3/NO_y, HCl/Cl_y, and BrO/Br_y upon volcanic aerosol amounts after the Pinatubo eruption have been used to identify the strong role of volcanic aerosol driven heterogeneous chemistry in controlling stratospheric O_3 loss [see review of *Solomon* 1999]. Figure 3 shows simulated annual mean radical ratios versus aerosol SAD at 50°N at 17 hpa (middle stratosphere) and 63 hPa (lower stratosphere) over 2006-2015 and 2091-2100 time periods in RCP8.5_novolc and RCP8.5_volc. Annual mean ClO/Cl_y and BrO/Br_y increase with increasing volcanic SAD in the lower and middle stratosphere while NO_x/NO_y decreases; ClO/Cl_y and BrO/Br_y increase more strongly in the near future when halogen loading is still high than in the future, particularly in the lower stratosphere. Similar dependencies are simulated for the southern mid-latitudes (not shown).

These changes in the partitioning of reactive halogens and NO_y are attributed to increased rates of heterogeneous reactions in the presence of volcanic SADs [*Fahey et al,.* 1993; *Granier and Brasseur,* 1992; *Koike et al.,* 1994; *Slusser et al.,* 1997; *Solomon et al.,* 1996; *Prather,* 1992; *Webster et al.,* 1998]. The key heterogeneous reactions on sulfate aerosols are:

$$N_2O_5 + H_2O \text{ (aerosol)} \rightarrow 2HNO_3 \quad (1)$$

$$ClONO_2 + H_2O \text{ (aerosol)} \rightarrow HOCl + HNO_3 \quad (2)$$

$$ClONO_2 + HCl \rightarrow HNO_3 + Cl_2 \quad (3)$$

$$BrONO_2 + H_2O \text{ (aerosol)} \rightarrow HNO_3 + HOBr \quad (4)$$

These reactions can proceed on polar stratospheric clouds (which form in extremely cold polar regions, especially Antarctica), even without volcanic sulfate aerosols, however, with enhanced aerosol surface areas, these reactions become more important in regions where temperatures are cold but not extremely cold [*Solomon et al.,* 1999 and references therein]. With increased SADs, the conversion of NO_x ($NO + NO_2$) to nitric acid (HNO_3), the primary NO_y reservoir species, is enhanced in RCP8.5_volc compared with RCP8.5_novolc, resulting in lower NO_x/NO_y and higher HNO_3/NO_x (Figure 3) for both the time periods. Reaction 1 is particularly efficient at changing the NO_x partitioning throughout the stratosphere as it is nearly temperature independent at stratospheric temperatures and water vapor [*Sander et al*., 2011]. A reduction in NO_x would be expected to reduce NO_x-catalyzed O_3 loss; however, these heterogeneous reactions also perturb halogen partitioning, enhancing the ClO_x- and BrO_x-catalyzed O_3 loss particularly in the 2006-2015 timeframe with elevated halogen levels in the atmosphere. Chlorine is activated directly via reactions 2 and 3 in which chlorine nitrate ($ClONO_2$) and hydrochloric acid (HCl), key chlorine reservoir species, are decomposed to produce reactive species. Chlorine is also activated indirectly by reaction 1 which reduces the amount of NO_2 available to combine with ClO to form $ClONO_2$. These reactions result in enhanced ClO/Cl_y in RCP8.5_volc compared to RCP8.5_novolc (Figure 3). The rates of reactions 2 and 3 increase with decreasing temperature hence these reactions compete more favorably in altering the chlorine partitioning in lower stratosphere than in middle stratosphere. Bromine is activated in a similar manner as chlorine via reactions 4 and 1 enhancing BrO/Br_y in the presence of volcanic aerosols (Figure 3). These reactions also enhance OH (not shown), contributing to HO_x-catalyzed O_3 loss. The net effect of changes in Cl_y, Br_y, and NO_y partitioning on O_3 is a balance between competing effects on NO_x, HO_x and halogen loss cycles, with net O_3 change depending on the altitude and atmospheric

241 halogen loading, consistent with the results of Tie and Brasseur [1995] using a two-dimensional
242 chemical transport model.

243 The presence of volcanic aerosols in conjunction with relatively high halogen loading in
244 the early 21st century enhances halogen-driven O_3 loss in the lower stratosphere and suppresses
245 the NO_x-catalyzed O_3 loss in the middle stratosphere, with the resulting O_3 changes as shown in
246 Figure 2. Since halogen loading diminishes to pre-anthropogenic levels by 2091-2100,
247 suppression of NO_x-catalyzed O_3 loss dominates in the presence of volcanic aerosols leading to
248 enhanced O_3 concentrations in RP8.5_volc relative to RCP8.5_novolc. Our results are consistent
249 with those of previous modeling studies that have analyzed the impact of volcanic aerosols
250 [*Granier and Brasseur*, 1992; *Tie and Brasseur*, 1995; *Solomon et al*., 1996; *Austin et al.,* 2013;
251 *Aquila et al.,* 2013] and the impact of geoengineering via sulfate aerosols [*Heckendorn et al.,*
252 2009; *Tilmes et al.,* 2009; *Pitari et al.,* 2014] on stratospheric O_3 in the presence of varying
253 amounts of halogens.

254

255 ## 4. Conclusions and Discussion

256 Analyses of three-member ensemble GFDL CM3 simulations indicate that the 21st
257 century evolution of stratospheric O_3 column (Figure 1) in response to a constant volcanic
258 aerosol distribution is a combination of opposing changes at different altitudes and halogen
259 levels (Figure 2). In the presence of volcanic aerosols the decrease in global mean stratospheric
260 O_3 column relative to 1980 levels is greater than that in their absence in the 2000-2020 period
261 due to the dominance of halogen-catalyzed O_3 loss in the lower stratosphere over the suppression
262 of NO_x-catalyzed O_3 loss in the middle stratosphere. However, the suppression of NO_x-catalyzed
263 O_3 destruction induced by volcanic aerosols dominates later in the 21st century as halogen levels

264 decline, resulting in global mean stratospheric O_3 recovering to 1980 levels about seven years
265 earlier relative to that in the absence of volcanic aerosols. In the mid-latitudes, the enhanced O_3
266 loss by halogens is nearly canceled out in terms of its effect of stratospheric O_3 column by the
267 NO_x-catalyzed suppression of O_3 loss in the presence of volcanic aerosols in the near future; by
268 2100 the NO_x suppression dominates, leading to stronger O_3 recovery (Figure 1c, d). Polar
269 stratospheric O_3 is most sensitive to the presence of volcanic aerosols. Strong O_3 column
270 reductions from enhanced halogen-catalyzed O_3 loss dominate over an extended period in the
271 21st century, resulting in delayed recovery to 1980 levels.

272 Our simulated total O_3 column changes in response to volcanic aerosols, particularly for
273 the early 21st century, depend strongly on the assumed aerosol loading since the suppression of
274 the NO_x catalytic cycle saturates with increasing SAD while the activation of the halogen and
275 HO_x catalytic cycles increases with SAD. The reduction in NO_x/NO_y ratio is saturated at the SAD
276 considered here [*Prather,* 1992; *Fahey et al.*, 1993]. Therefore, a greater SAD (or an episodic
277 intense volcanic eruption with high SAD) in the future is unlikely to lead to further changes in
278 NO_x/NO_y ratio or middle stratospheric O_3. Because the increase in ClO/Cl_y (and BrO/Br_y) is not
279 saturated at the SAD considered here, greater SAD, particularly at present-day halogen levels,
280 can lead to greater increases in ClO/Cl_y and thus stronger lower stratospheric O_3 reductions that
281 could outweigh the middle stratospheric O_3 increases, resulting in stronger decreases in
282 stratospheric O_3 column in the early 21st century.

283 Additionally, our results depend on our modeling framework and its deficiencies. For
284 example, CM3 does not explicitly simulate the stratospheric aerosol formation, growth and loss
285 processes after volcanic eruptions – processes that determine the aerosol SAD and therefore
286 affect the rate of heterogeneous reactions. We also do not consider trends in halogenated very

short-lived substances that can contribute to halogen loading of the stratosphere [*Montzka et al.*, 2011] and can counteract the O_3 column increases in the future from NO_x suppression at elevated volcanic aerosol levels. Similar experiments with other global models that include these processes will help provide more robust estimates of the impact of stratospheric volcanic aerosols on the evolution of stratospheric O_3 in the future.

The analysis presented here underscores the importance of volcanic aerosols in altering the future projection of stratospheric O_3. Predicting future volcanic eruptions on a global scale and the resulting stratospheric aerosol distributions is nearly impossible as of now. Model simulations that consider hypothetical volcanic aerosol distributions based on recent measurements could help provide a lower limit of the influence of volcanic aerosols on stratospheric O_3. Further, the response of stratospheric O_3 column to observed SAD over the 2000-2010 period for which we have observational constraints can help provide estimates of the net effect of recent observed SAD on total O_3 column.

5. Acknowledgments

We are grateful to David Paynter, and John Wilson for helpful discussions. We thank Pu Lin and Ron Stouffer for constructive comments on an earlier version of the manuscript. All data used in this study can be obtained by contacting the corresponding author (Vaishali.Naik@noaa.gov).

6. References

Aquila, V., L D. Oman, R. Stolarski, A. R. Douglass, and P. A. Newman (2013), *J. Atmos. Sci.*, 70, 894-900, doi:10.1175/JAS-D-12-0143.1.

Austin, J., L. W. Horowitz, M. D. Schwarzkopf, R. J. Wilson, and Hiram Levy II (2013), Stratospheric ozone and temperature simulated from the preindustrial era to the present day, *J. Climate,* **26**, 3528-3542, doi:10.1175/JCLI-D-12-00162.1.

Austin, J. and R. J. Wilson (2010), Sensitivity of polar ozone to sea surface temperatures and halogen amounts, *J. Geophys. Res*., **115**, D18303, doi:10.1029/2009JD013292.

Bekki et al. (2011), Future ozone and its impact on surface UV, Chapter 3 in *Scientific Assessment of Ozone Depletion: 2010,* Global Ozone Research and Monitoring Project – Report No. 52, 516pp., World Meteorological Organization, Geneva, Switzerland.

Brasseur, G. P., et al. (1999), Atmospheric Chemistry and Global Change, Oxford University Press Inc., NY, USA.

Collins, M., et al. (2013), Long-term Climate Change: Projections, Commitments and Irreversibility, in: *Climate Change 2013: The Physical Science Basis. Contribution of Working Group I to the Fifth Assessment Report of the Intergovernmental Panel on Climate Change* [Stocker, T. F., D. Qin, G.-K. Plattner, M. Tignor, S. K. Allen, J. Boschung, A. Nauels, Y. Xia, V. Bex and P. M. Midgley (eds.)]. Cambridge University Press, Cambridge, United Kingdom and New York, NY, USA.

Donner, L. J., et al. (2011), The dynamical core, physical parameterizations, and basic simulation characteristics of the atmospheric component of AM3 of the GFDL global coupled model CM3, *J. Climate*, **24**, 3484-3519.

Eyring, V., et al. (2010), Sensitivity of 21st century stratospheric ozone to greenhouse gas scenarios, *Geophys. Res. Lett.,* **37**, L16807, doi:10.1029/2010GL044443.

Eyring, V., et al. (2013), Long-term ozone changes and associated climate impacts in CMIP5 simulations, *J. Geophys. Res*., **118**, 1-32, doi:10.1002/jgrd.50316.

Fahey, D. W., et al. (1993), In situ measurements constraining the role of sulphate aerosols in mid-latitude ozone depletion, *Nature*, 363, 509-514.

Fyfe J. C., K. von Salzen, J. N. S. Cole, N. P. Gillett, and J.-P. Vernier (2013), Surface response to stratospheric aerosol changes in a coupled atmosphere–ocean model, *Geophys. Res. Lett.*, **40**, 584–588, doi:10.1002/grl.50156.

Granier, C., and G. Brasseur (1992), Impact of heterogeneous chemistry on model predictions of ozone changes, *J. Geophys. Res.*, **97**(D16), 18015–18033, doi:10.1029/92JD02021.

Heckendorn, P., et al. (2009), The impact of geoengineering aerosols on stratospheric temperature and ozone, *Environ. Res. Lett.*, **4**, doi:10.1088/1748-9326/4/4045108.

Hofmann, D., J. Barnes, M. O'Neill, M. Trudeau, and R. Neely (2009), Increase in background stratospheric aerosol observed with lidar at Mauna Loa Observatory and Boulder, Colorado, *Geophys. Res. Lett.*, **36**, L15808, doi:10.1029/2009GL039008.

Junge, E., C. W. Chagnon, and J. E. Manson (1961), A world-wide stratospheric aerosol layer, *Science*, **133**, 1478–1479, doi:10.1126/science.133.3463.1478-a.

John, J., A. M. Fiore, V. Naik, L. W. Horowitz, and J. Dunne (2012), Climate versus emission drivers of methane lifetime from 1860 to 2100, *Atmos. Chem. Phys*., **12**, 12021-12036, doi:10.5194/acp-12-12021-2012.

Koike, M. et al. (1994), Impact of Pinatubo aerosols on the partitioning between NO_2 and HNO_3, *Geophys. Res. Lett.*, **21**, 597-600.

Lary, D. J., M. P. Chipperfield, R. Toumi, and T. Lenton (1996), Heterogeneous atmospheric bromine chemistry, *J. Geophys. Res.*, **101**, 1489-1504.

McCormick, P. M., L. W. Thomason, and C. Trepte (1995), Atmospheric effects of the Mt. Pinatubo eruption, *Nature*, **373**, 399–404, doi:10.1038/373399a0.

354 Montzka, S. A., et al. (2011), Ozone-Depleting Substances (ODSs) and Related Chemicals
355 Chapter 1 in *Scientific Assessment of Ozone Depletion: 2010, Global Ozone Research and*
356 *Monitoring* Project-Report No. 52, 516 pp., World Meteorological Organization, Geneva,
357 Switzerland, 2011.
358 Naik, V., et al. (2013), Impact of preindustrial to present-day changes in short-lived pollutant
359 emissions on atmospheric composition and climate forcing, *J. Geophys. Res*., **118**, 8086–
360 8110, doi:10.1002/jgrd.50608.
361 Pitari, G., V. Aquila, B. Kravitz, A. Robock, S. Watanabe, I. Cionni, N. De Luca, G. Di Genova,
362 E. Mancini, and S. Tilmes (2014), Stratospheric ozone response to sulfate geoengineering:
363 Results from the Geoengineering Model Intercomparison Project (GeoMIP), *J. Geophys.*
364 *Res.*, **119**, 2629–2653, doi:10.1002/2013JD020566.
365 Prather, M. (1992), Catastrophic loss of stratospheric ozone in dense volcanic clouds, *J.*
366 *Geophys. Res.*, **97**, 10187–10191, doi:10.1029/92JD00845.
367 Riahi, K. et al. (2011), RCP8.5 – A scenario of comparatively high greenhouse gas emissions,
368 *Clim. Change.,* **109**, 33-57, 10.1007/s10584-011-0149-y.
369 Sander, S. P., J. Abbatt, J. R. Barker, J. B. Burkholder, R. R. Friedl, D. M. Golden, R. E. Huie, C.
370 E. Kolb, M. J. Kurylo, G. K. Moortgat, V. L. Orkin and P. H. Wine (2011), Chemical Kinetics
371 and Photochemical Data for Use in Atmospheric Studies, Evaluation No. 17, JPL Publication
372 10-6, Jet Propulsion Laboratory, Pasadena, http://jpldataeval.jpl.nasa.gov.
373 Santer, B.D., et al. (2012), Identifying human influences on atmospheric temperature, *PNAS*,
374 doi:10.1073/pnas.1210514109.
375 Santer, B. D., et al. (2014), Volcanic contribution to decadal changes in tropospheric temperature,
376 *Nature*, **7**, 185-189, doi:10.1038/ngeo2098.

377 Slusser, J. R., D. J. Fish, E. K. Strong, R. L. Jones, H. K. Roscoe, and A. Sarkissian (1997), Five
378 years of NO_2 vertical column measurements at Faraday (65°S): Evidence for the hydrolysis
379 of $BrONO_2$ on Pinatubo aerosols, *J. Geophys. Res.*, **102**(D11), 12987–12993,
380 doi:10.1029/97JD00359.
381 Solomon, S., R. W. Portmann, R. R. Garcia, L. W. Thomason, L. R. Poole, and M. P. McCormick
382 (1996), The role of aerosol variations in anthropogenic ozone depletion at northern
383 midlatitudes, *J. Geophys. Res.*, **101**, 6713–6727, doi:10.1029/95JD03353.
384 Solomon, S. (1999), Stratospheric ozone depletion: A review of concepts and history, *Rev.*
385 *Geophys.*, **37**, 275–316, doi:10.1029/1999RG900008.
386 Sato, M., J. E. Hansen, M. P. McCormick, J. B. Pollack (1993), Stratospheric aerosol optical
387 depths, 1850–1990, *J. Geophys. Res*., **98**, 22987–22994.
388 Stenchikov, G. L., I. Kirchner, A. Robock, H.-F. Graf, J. C. Antuna, R. G. Grainger, A. Lambert,
389 and L. Thomason (1998), Radiative forcing from the 1991 Mount Pinatubo volcanic
390 eruption, *J. Geophys. Res.*, **103**, 13,837–13,858, doi:10.1029/98JD00693.
391 Tilmes, S., R. R. Garcia, D. E. Kinnison, A. Gettelman, and P. J. Rasch (2009), Impact of
392 geoengineered aerosols on the troposphere and stratosphere, *J. Geophys. Res.*, **114**, D12305,
393 doi:10.1029/2008JD011420.
394 Thomason, L. W., L. R. Poole, and T. Deshler (1997), A global climatology of stratospheric
395 aerosol surface area density deduced from Stratospheric Aerosol and Gas Experiment II
396 measurements: 1984–1994, *J. Geophys. Res*., **102**, 8967–8976, doi:10.1029/96JD02962.
397 Tie, X. X., and G. P. Brasseur (1995), The response of stratospheric ozone to volcanic eruptions:
398 sensitivity to atmospheric chlorine loading, *Geophys. Res. Lett.*, **22**, 3035-3038, doi:
399 10.1029/95GL03057.

SPARC Assessment of stratospheric aerosol properties (ASAP) (2006), Technical report WCRP-124/WMO/TD-No. 1295/SPARC report no. 4, SPARC, Toronto, Ontario, CA, pp. 322.

Vernier, J. P., et al. (2009), Tropical stratospheric aerosol layer from CALIPSO lidar observations, *J. Geophys. Res.*, **114**, D00H10, doi:10.1029/2009JD011946.

Vernier, J.-P., et al. (2011), Major influence of tropical volcanic eruptions on the stratospheric aerosol layer during the last decade, *Geophys. Res. Lett.*, **38**, L12807, doi:10.1029/2011GL047563.

Webster, C. R., et al. (1998), Evolution of HCl concentrations in the lower stratosphere from 1991 to 1996 following the eruptions of Mt. Pinatubo, *Geophys. Res. Lett.*, **25**(7), 995-998.

Wennberg, P. O., et al. (1994), Removal of stratospheric O_3 by radicals: In situ measurements of OH, HO_2, NO, NO_2, ClO, and BrO, *Science*, 266, 398-404.

7. Figures

Figure 1. The 1980 baseline-adjusted time series of stratospheric O_3 column (200 – 0 hPa) from 1960 to 2100 for the RCP8.5_novolc and RCP8.5_volc simulations for (a) global and annual average, (b) annual average over 25°N-25°S (c) annual average over 35°-60°N (d) annual average over 35-60°S (e) averaged over 60-90°N for March, and (f) averaged over 60-90°S for October. Shaded areas indicate ± 1-standard deviation across the three ensemble members for each simulation. The time series are smoothed with a 1:2:1 filter applied 30 times iteratively.

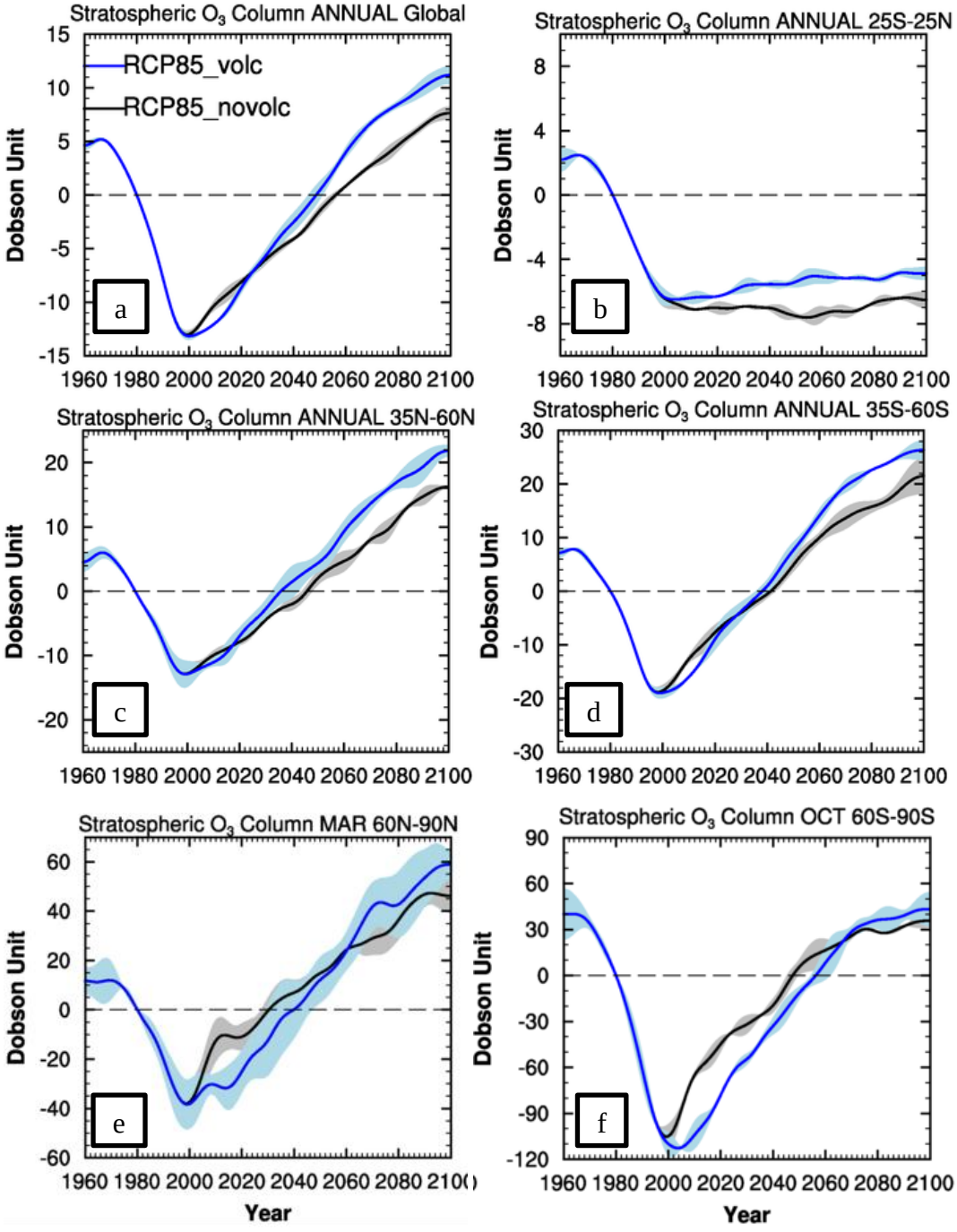

Figure 2. Change in zonal mean O_3 concentration for RCP8.5_volc with respect to RCP8.5_novolc annual (top), March (middle) and October (bottom) for mean 2006-2015 (left) and 2091-2100 (right) time periods. Stippled areas show differences that are significant at 95% confidence level based on student's t-test.

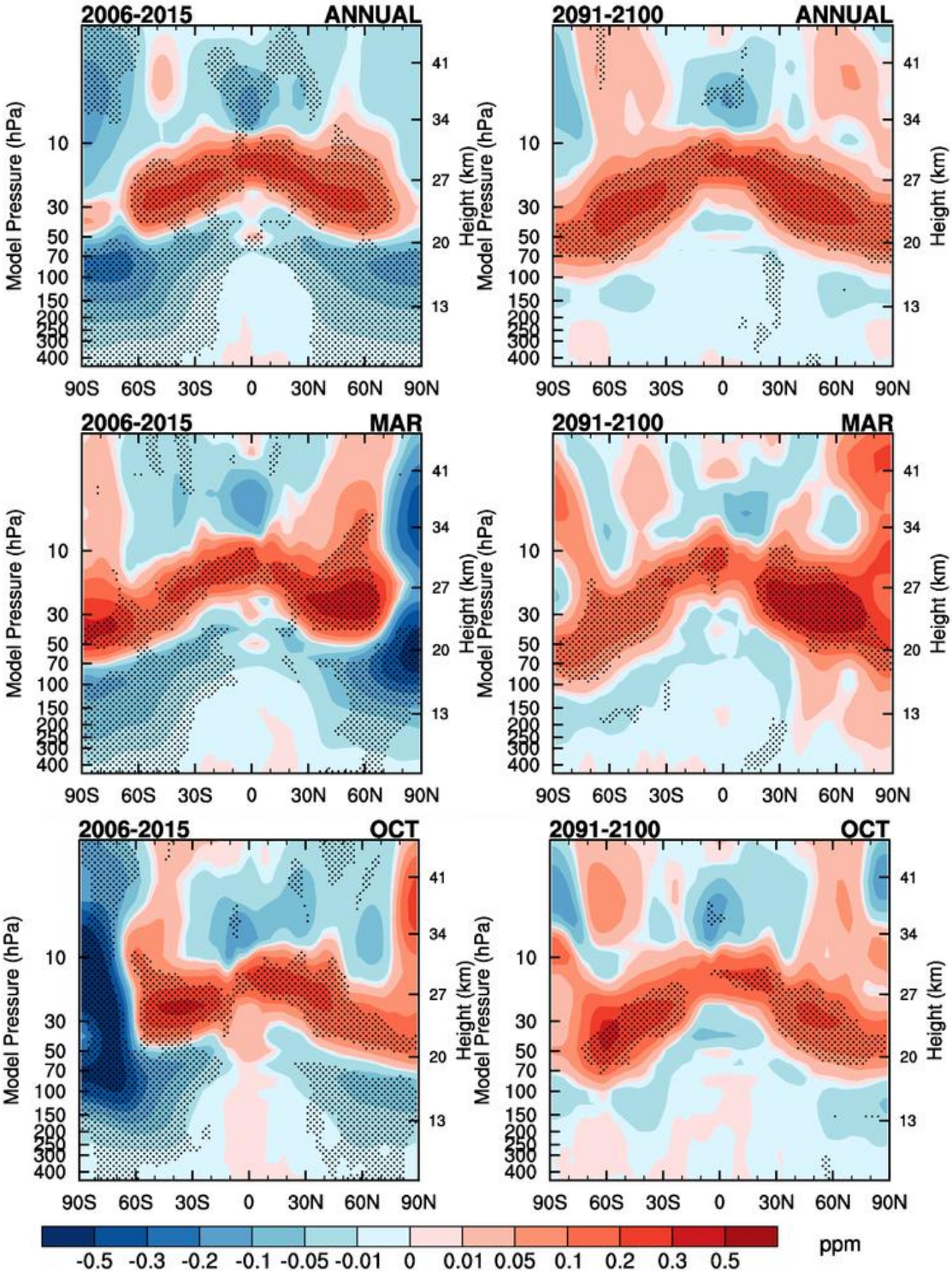

Figure 3. Annual mean radical ratios as a function of volcanic aerosol surface area density for 17hPa and 63hPa at 50°N. Values are individual years within 2006-2015 and 2091-2100 time periods averaged over three ensemble members of the RCP8.5_novolc and RCP8.5_volc simulations.

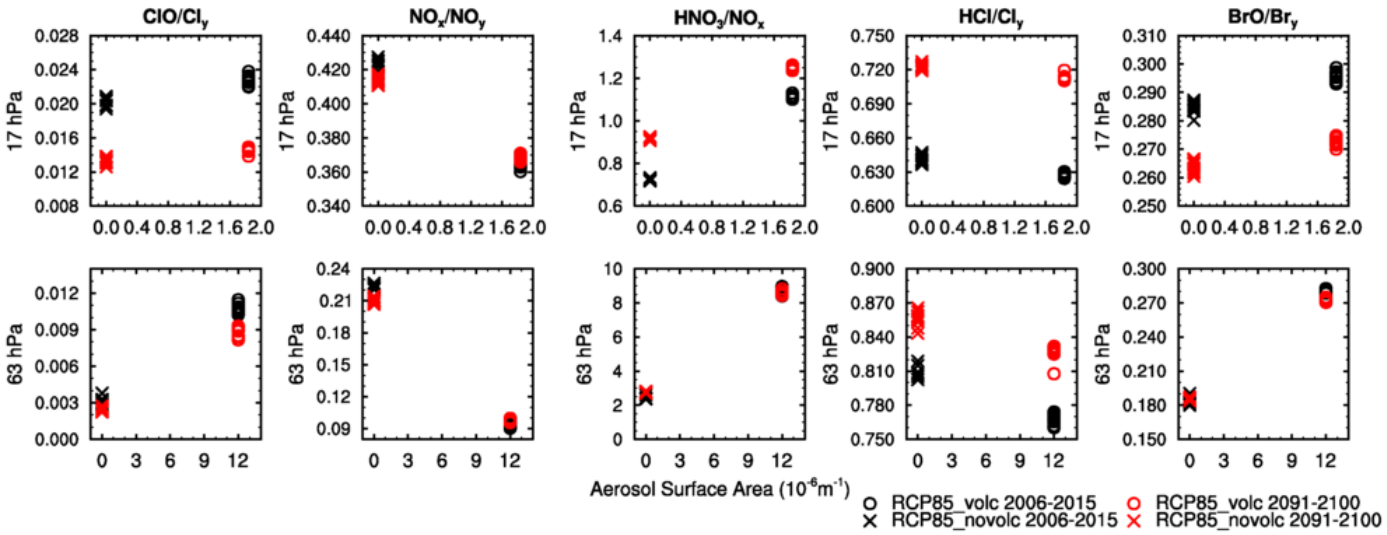

Auxiliary Material for

Impact of Volcanic Aerosols on Stratospheric Ozone Recovery

Vaishali Naik[1], Larry W. Horowitz[2], and M. Daniel Schwarzkopf[2]

[1] UCAR/NOAA Geophysical Fluid Dynamics Laboratory, Princeton, NJ 08540

[2] NOAA Geophysical Fluid Dynamics Laboratory, Princeton, NJ 08540

Geophysical Research Letters, 2014

Figure S1. Annual mean zonal average volcanic aerosol surface area density in RCP8.5_volc simulations.

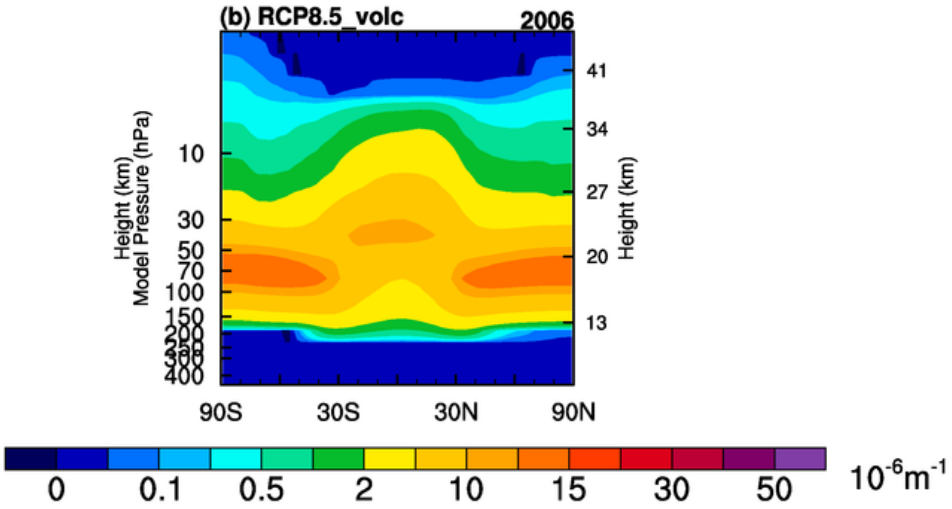

Figure S2. 1980 baseline-adjusted trend in annual mean equivalent stratospheric chlorine (ESC = $Cl_y + 60* Br_y$) at 63 hPa.